

Intelligent Spatial Perception by Building Hierarchical 3D Scene Graphs for Indoor Scenarios with the Help of LLMs*

Yao Cheng^{1,2}, Zhe Han², Fengyang Jiang^{1,2}, Huaizhen Wang^{1,2}, Fengyu Zhou³, Qingshan Yin², and Lei Wei²

Abstract—This paper addresses the high demand in advanced intelligent robot navigation for a more holistic understanding of spatial environments, by introducing a novel system that harnesses the capabilities of Large Language Models (LLMs) to construct hierarchical 3D Scene Graphs (3DSGs) for indoor scenarios. The proposed framework constructs 3DSGs consisting of a fundamental layer with rich metric-semantic information, an object layer featuring precise point-cloud representation of object nodes as well as visual descriptors, and higher layers of room, floor, and building nodes. Thanks to the innovative application of LLMs, not only object nodes but also nodes of higher layers, e.g., room nodes, are annotated in an intelligent and accurate manner. A polling mechanism for room classification using LLMs is proposed to enhance the accuracy and reliability of the room node annotation. Thorough numerical experiments demonstrate the system’s ability to integrate semantic descriptions with geometric data, creating an accurate and comprehensive representation of the environment instrumental for context-aware navigation and task planning.

I. INTRODUCTION

The advancement of intelligent robot navigation calls for a paradigm shift from mere geometric mapping to a more comprehensive understanding of spatial environments. Current widely adopted mapping techniques [1], [2], [3] rely solely on geometric information and thus fail to capture the rich semantic context required for truly intelligent navigation. 3D Scene Graphs (3DSGs) [4], [5], [6], [7] have emerged as a powerful representation of spatial environments that provide a structured and comprehensive understanding of both the geometric and semantic aspects of a scene. Therefore, they find applications in the field of robotics for tasks such as navigation, object manipulation, and scene interpretation [8], [6], [9], [10].

Early works, such as [4], [5], presented the first 3DSG construction frameworks and validated the idea of generating a graph spanning an entire building and incorporating rooms as well as objects detected together with the spatial relationships of these entities. The concept of spatial perception for robotics was first introduced in [7], where the significance of a hierarchical structure for a 3DSG was addressed and an advanced spatial perception system, as a collection of

algorithms designed to generate 3DSGs with sensor data in real-time was developed [7]. These works have laid the conceptual foundation for subsequent research in 3DSGs, emphasizing their significance in Artificial Intelligence (AI) and the field of robotics.

The advent of Large Language Models (LLMs) [11], [12] and Large Visual Language Models (LVLMs) [13], [14] has been a catalyst in advancing the capabilities of 3DSGs. The synergy between LLMs and spatial understanding holds the potential to transform the way robots perceiving and interacting with their environments. Recent studies [6] have begun to explore the fusion of LLMs with 3DSGs, demonstrating the potential for enhanced task planning and navigation. The ability to describe node attributes and relationships within the graph using natural language is a pivotal advancement, facilitating seamless integration with AI systems that can generate and interpret human-like text. However, the authors [6] only address the construction of an object-centric single-layer 3DSG, leaving the advantages of LLMs in establishing scalable hierarchical 3DSGs unexploited.

Building upon this rich body of literature, this paper introduces a novel system that leverages the power of LLMs to construct hierarchical 3DSGs for intelligent spatial perception in indoor scenarios. We outline a method for constructing 3DSGs that encompass a fundamental layer with metric-semantic information, an object layer with visual descriptors as well as point-cloud representations, and higher layers representing areas or regions, culminating in scalable representations through room, floor, and building nodes. LLMs are leveraged to annotate not only object nodes but also nodes of higher layers, e.g., room nodes. In particular, a polling mechanism for room classification using LLMs is proposed to improve the accuracy and reliability of the room node annotation. As a byproduct, a nice problem formation of constructing 3DSGs and exploiting LLMs as a tool is established for future research in this area. Thorough experiments show that, by harnessing the capabilities of LLMs, our system is able to integrate semantic descriptions with geometric data and to create an accurate and comprehensive representation of an indoor environment that is instrumental for intelligent agent navigation and task planning.

II. METHOD

A. Problem formulation

The hierarchical nature of 3DSGs allows for the representation of complex scenes at various levels of abstraction, from individual objects to entire rooms or buildings [5], [7]. Here we denote a 3DSG consisting of K hierarchical layers

*This research was funded by Key R&D Program of Shandong Province, China of grant number 2023CXPT094 and the Jinan City and University Cooperation Development Strategy Project under Grant JNSX2023012.

¹Shandong New Generation Information Industrial Technology Research Institute, Jinan, 250100, Shandong, P. R. China chengyao01, jiangfy, wanghuaizhen@inspur.com

²Inspur Intelligent Terminal Co., Ltd., Jinan, 250100, Shandong, P. R. China hanzhe, yingqsh, weilei03@inspur.com

³School of Control Science and Engineering, Shandong University, Jinan, 250061, Shandong, P. R. China zhoufengyu@sdu.edu.cn

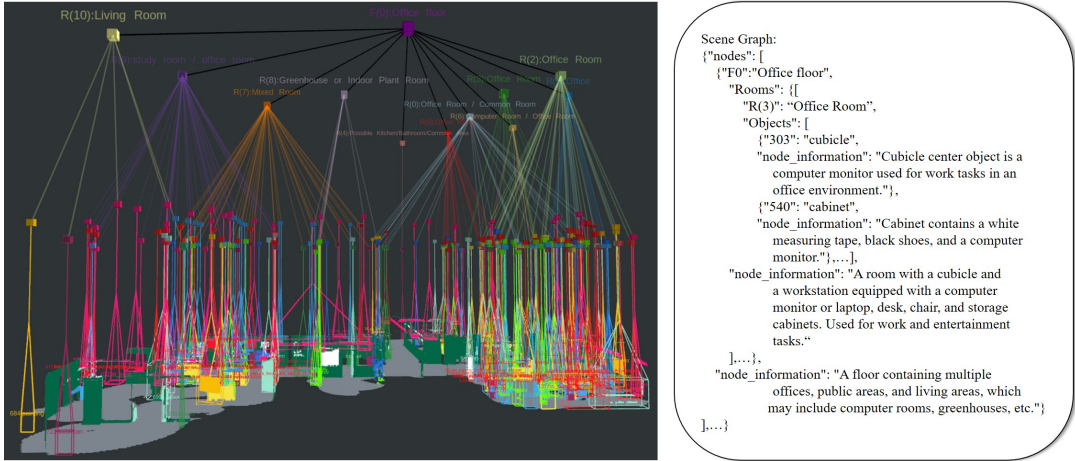


Fig. 1: Illustration of the proposed hierarchical 3DSG

as $\mathcal{G} = (\mathcal{V}, \mathcal{E})$ [4], [5], [7], where \mathcal{V} represents the set of nodes belonging to the K layers, i.e., $\mathcal{V} = \cup_{k=1}^K \mathcal{V}_k$ with \mathcal{V}_k containing the M_k nodes of the k -th layer

$$\mathcal{V}_k = \{v_{k,1}, v_{k,2}, \dots, v_{k,M_k}\}, \quad (1)$$

and $v_{k,j}$ denoting the j -th node ($j = 1, 2, \dots, M_k$) of the k -th layer. Each node is annotated by a set of descriptions, i.e., for node $v_{k,j}$

$$\mathcal{C}_{k,j} = \{c_{k,j}^{(1)}, c_{k,j}^{(2)}, \dots, c_{k,j}^{(L_{k,j})}\}, \quad (2)$$

consisting of $L_{k,j}$ attributes covering multiple perspectives and dimensions. These pieces of information serve as the basis for intelligent agent navigation and task planning. For instance, the attributes of object nodes include descriptions that distinguish “operable” objects including various small items such as cups and food from assets like furniture and home appliances that an intelligent agent generally cannot move.

The whole set of edges in the 3DSG \mathcal{G} is represented by \mathcal{E} . Each edge connects two nodes within the same layer or two nodes belonging to adjacent layers, i.e., an edge stemming from node $v_{k,j}$ of the k -th layer connects only nodes in $\mathcal{V}_{k-1} \cup \mathcal{V}_k \cup \mathcal{V}_{k+1}$ [7].

B. Construction of 3DSGs

This section delves into the generation of hierarchical 3DSGs with the help of LLMs. Focusing on indoor scenarios, we propose a multi-tier structure of the 3DSG illustrated in Figure 1. We call *Layer-1* a fundamental layer taking the form of a 3D mesh and holding crucial metric-semantic information required for the construction of upper layers of the 3DSG and navigation tasks. In parallel to building *Layer-1*, object nodes are initiated and gradually equipped with rich geometric as well as semantic descriptions, forming *Layer-2*. In *Layer-3*, object nodes are grouped, populating the concept of areas or regions of the scenario that the 3DSG is describing. By resorting to LLMs, the resulting areas are annotated based on the attributes of the object nodes they contain. *Layer-4* and *Layer-5* are designed to hold “floor” and

“building” nodes, respectively, which are particularly useful for generating a scalable and well-organized representation of, e.g., large multi-functional venues.

1) *Layer-1 - Fundamental layer*: As the first layer of the 3DSG, we construct a metric-semantic 3D mesh. A visual-inertial [15] or a LiDAR-visual-inertial odometry pipeline [2], [3], is available as a common practice. For each RGB-D frame¹ coming in, we first employ the 2D semantic segmentation network² YOLOv8 [16] to achieve a pixel-level semantic segmentation of the RGB image. This semantic segmentation and depth information are then converted into a semantically annotated 3D point cloud, which is adjusted based on the robot’s pose estimate, i.e., it is transformed from the coordinate system of the camera to the world coordinate system. On the one hand, this semantically labeled point cloud is integrated into a Truncated Signed Distance Field (TSDF) via a ray-casting process [7]. The resulting voxel-based map is equipped with data indicating the availability of free space and a probabilistic distribution of potential semantic labels for each voxel [15]. Via the marching cubes algorithm, the voxel map is transformed into a 3D mesh [7]. On the other hand, the aforementioned point cloud is used to construct object nodes of *Layer-2* as discussed in detail in Section II-B.2.

In addition to the 3D mesh used also for the visualization purpose, *Layer-1* contains a “hidden” sub-layer which plays an essential role in building the room layer described in Section II-B.3. It takes the form of a sparse graph of places as first introduced in [7], where a Generalized Voronoi Diagram (GVD) of the environment is computed based on the 3D mesh and approximated to form the graph of places as a representation of obstacle-free spots and their connectivity.

2) *Layer-2 - Object layer*: In Section II-B.1, where the construction of the fundamental layer is detailed, the point

¹Depending on the type of cameras used, the depth images could be directly provided by an RGB-D camera or retrieved through the stereo matching in the case of a stereo camera.

²Class-agnostic segmentation models can also be employed to achieve open-vocabulary detection and segmentation [6].

cloud retrieved from each entire data frame is used to build up a global map to thoroughly represent the spatial structure of the environment. For *Layer-2*, nevertheless, the point cloud is extracted on the “segmentation-mask” basis and used to initiate a new object node or to improve the representation of an existing one. The corresponding mask serves as the input of a visual feature extractor such as CLIP [14] to generate a visual descriptor. Consequently, the point cloud together with the visual descriptor are taken as the geometric and semantic representation of each object instance. By leveraging both geometric and semantic similarity metrics [6], the association of these object instances is conducted. Finally, for an object node $v_{2,j}$ of *Layer-2* ($k=2$), the point cloud of its various instances is fused into its unique point-cloud representation $\mathbf{P}_{2,j}^{(o)}$, whereas a semantic feature vector $\mathbf{f}_{2,j}^{(o)}$ is obtained likewise through the object instance fusion [6].

Subsequently, with the help of an LVLM and an LLM, node attributes are generated. Based on the RGB image of each object instance, an LVLM is first used to produce an initial set of object descriptions covering the following aspects:

- Object state: The current condition or status of an object (e.g., switched on or off, orientation).
- Predicates: Descriptive statements that relate objects and their attributes (e.g., “the cup is on the table”).
- Affordances: Action possibilities presented by objects based on their properties (e.g., “a chair can be sat on”).
- Other attributes: Detailed characteristics of objects that can influence task planning and execution.

The prompts for the LVLM are adapted according to observations and findings in navigation tasks where 3DSGs are used. Along with the object association and fusion, an LLM represented by ϕ_{LLM} is prompted to provide a summary of the descriptions associated with the object instances belonging to the same object node, i.e.,

$$C_{2,j} = \phi_{\text{LLM}} \left(C_{2,j}^{(\text{LVLM},1)}, \dots, C_{2,j}^{(\text{LVLM},N_{2,j})}, P_{2,j} \right), \quad (3)$$

where $C_{2,j}^{(\text{LVLM},i)}$ ($i=1, \dots, N_{2,j}$) denotes the node description obtained via the LVLM in the i -th instance of the j -th object node of *Layer-2*, and $P_{2,j}$ represents the prompt tailored for the LLM to output a desired summary of the node description.

Note that the procedure of node captioning described above can be carried out in real-time by calling the API of an LVLM and an LLM. In addition, we have an offline alternative [6] in our implementation as well based on the sequence of RGB images saved. It is particularly useful for cases where the LVLM and the LLM are deployed and run locally on the intelligent agent. Moreover, it can also be treated as a separate module used to supplement and enrich the node attributes of an exiting 3DSG [5] providing that the raw data is available or can be extracted from an environment [17].

Compared to the object layer of Hydra [7], the geometric representation of the object nodes in *Layer-2* of our proposed

3DSG is more accurate and thus more suitable for robotic manipulation tasks. In addition, each node is enriched with a semantic descriptor and a comprehensive set of attributes derived through LLM-based analysis, which are crucial for intelligent task planning.

3) *Room layer and upper layers*: Though intuitive and straightforward for human-beings, room identification is a non-trivial robotic perception task. To initiate the construction of the room layer, we segment the rooms based on the sub-layer of *Layer-1* described in Section II-B.1 by clustering this sparse graph of places using persistent homology [7]. Once the room identification is done, we propose to categorize and annotate the rooms by prompting an LLM to infer their functional and structural characteristics based on the object nodes of *Layer-2*. In this way, the description set of the ℓ -th room node of *Layer-3* is obtained as

$$C_{3,\ell} = \phi_{\text{LLM}} \left(\bigcup_{j \in \mathcal{S}_{3,\ell}^{(o)}} C_{2,j}, P_{3,\ell} \right) \quad (4)$$

where $\mathcal{S}_{3,\ell}^{(o)}$ represents an index set of object nodes of *Layer-2* belonging to the ℓ -th room node $v_{3,\ell}$, and $P_{3,\ell}$ symbolizes the prompt template designed for the LLM to deduce a room type and perform room node captioning based on the object nodes that room node $v_{3,\ell}$ contains (cf. Figure 9(a) for an example where the LLM is guided to infer a room type).

Annotating room nodes featuring typical functional characteristics with explicit labels facilitates down-streaming planning tasks [7]. In addition, the token size can be reduced, and providing the LLM with concise and explicit information prevents it from hallucinating. Inaccurate node annotation, on the other hand, can be misleading, resulting in planning failures. Hence, we propose a polling mechanism that leverages the LLM’s own capabilities to resolve issues with hallucination as well as uncertainty and to effectively identify multi-functional segments of an indoor environment that should be annotated with a concise description instead. To this end, given a set of typical room labels of size N

$$C^{(\text{typ})} = \left\{ c_1^{(\text{label})}, c_2^{(\text{label})}, \dots, c_N^{(\text{label})} \right\}, \quad (5)$$

we query the LLM for L rounds and obtain the polling results as follows

$$\mathbf{p}_\ell = \sum_{i=1}^L \phi_{\text{LLM}}^{(i)} \left(\bigcup_{j \in \mathcal{S}_{3,\ell}^{(o)}} C_{2,j}, C^{(\text{typ})}, P_{3,\ell}^{(\text{label})} \right), \quad (6)$$

where $\mathbf{p}_\ell = [p_{\ell,1} \ p_{\ell,2} \ \dots \ p_{\ell,N}]^T$ with $p_{\ell,n}$ representing for how many times of the L query rounds, the typical room label $c_n^{(\text{label})}$ is selected, and $P_{3,\ell}^{(\text{label})}$ is the corresponding prompt template. As discussed in detail in Section III-C, for indoor household scenarios, the set of typical room labels are determined empirically by evaluating 483 rooms of the Stanford 3D Scene Graph dataset [5].

Based on findings of a through investigation shown in Section III-C, we propose to annotate room node $v_{3,\ell}$ with $c_n^{(\text{label})}$ only when $p_{\ell,n} = L$, i.e., for all L rounds of querying

the LLM, $c_n^{(\text{label})}$ is suggested as the room label for $v_{3,\ell}$. This strategy guarantees the accuracy of the room labels incorporated in the 3DSG to a large extent and in the meantime effectively identifies multi-functional segments of the scenario, where a description provides more insights into down-streaming navigation tasks compared to a single label. Moreover, sometimes the identified room areas might not have stand-out or widely acknowledged functionality characteristics, at least not according to the object nodes they contain, e.g., lobbies, corridors, closets. Therefore, for all these cases, a room label is not explicitly provided in the 3DSG, and instead a concise version of the room node description is included which is able to supply subsequent robotic tasks with useful and unambiguous information.

For the construction of upper layers of the 3DSG, taking the floor layer as an example, we cluster rooms with a similar height determined with the poses of the object nodes they contain and form a floor layer. Then the LLM is guided to annotate the resulting floor node based on the room nodes of this floor. In the case of multi-storey high-rise buildings, a robotic agent usually travels with an elevator to reach a certain floor, and the 3DSG of each floor might have to be constructed separately. Floor layers are naturally identified with a-priori knowledge of the environment.

C. Data structure of 3DSGs

To leverage the capabilities of LLMs for down-streaming navigation tasks, 3DSGs are represented as a NetworkX graph object [18], [9] in a JSON data format in a text-serialized manner as depicted in Figure 1. By converting the 3DSG into JSON, it becomes a structured input that can be directly utilized by LLMs for various AI tasks, such as semantic search and planning for robotic navigation [9].

III. EXPERIMENTAL RESULTS

The primary goal of our experiments is to validate the effectiveness of the proposed method of generating hierarchical 3DSGs. If not stated otherwise, the ERNIE 3.5 model provided by Baidu is utilized for the numerical experiments, with the temperature parameter set to 0.1 to ensure stable responses.

A. 3DSG generation

We illustrate the 3DSG of the office scene of the uHumans2 dataset [19] generated with the proposed method already in Figure 1. The point cloud of the object nodes is not shown in this whole view of the 3DSG for clarity of the visualization. Figure 2 presents a few examples and a comparison with their counterparts taking the form of a mesh as in the Hydra framework [7]. It can be seen that this point-cloud form serves as a more precise representation of the object nodes, which is essential for guaranteeing a satisfactory robot navigation and manipulation performance.

In addition to testing with datasets, we have also constructed 3DSGs in real-time with a wheeled robot developed in our company for indoor scenarios. Data is collected using a combination of visual and LiDAR sensors, providing the

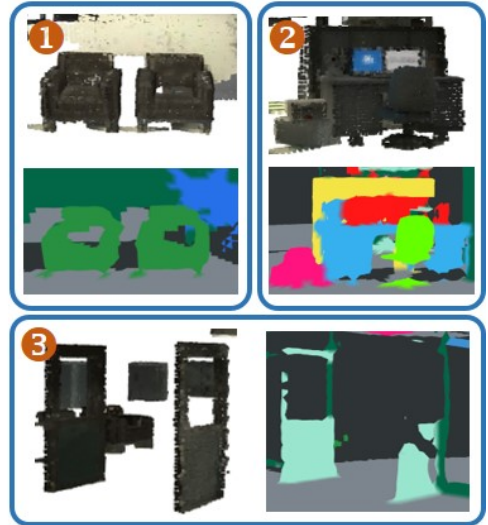


Fig. 2: Examples and comparison of point-cloud and mesh representations of object nodes

necessary geometric and semantic information for constructing the 3DSGs. In particular, we use the ORBBEC Femto Bolt RGB-D camera to obtain RGB and depth images of the scenario. Coupling a 2D LiDAR sensor, a wheel odometry, and an inertial measurement unit (IMU) [2] equipped on the robot device leads to pose estimates essential for the generation of *Layer-1*. The 2D semantic segmentation network YOLOv8 is employed for pixel-level semantic segmentation of the RGB images. Figure 3 presents the resulting 3DSG created for an office scene of our company. It consists of a fundamental layer, an object layer, a room layer, and a floor layer with nodes annotated. In summary, these results

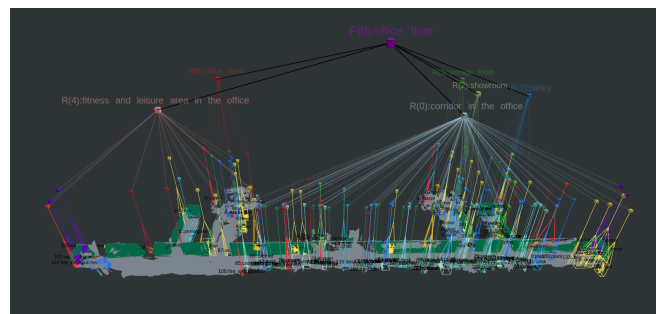


Fig. 3: 3DSG of an office scenario constructed in real-time with a wheeled robot

indicate that with the proposed scheme, 3DSGs can be built using not only existing datasets but also on-board sensors of a robotic device in real-time.

Although preliminary results of applying the 3DSG shown in Figure 3 for robot navigation in the corresponding office scene are not shown due to the page limitation, the performance is satisfactory. On the other hand, it should be noted that there are still not any standardized or widely acknowledged evaluation criteria and metrics for 3DSGs. Generally speaking, the geometric accuracy of the fundamental layer

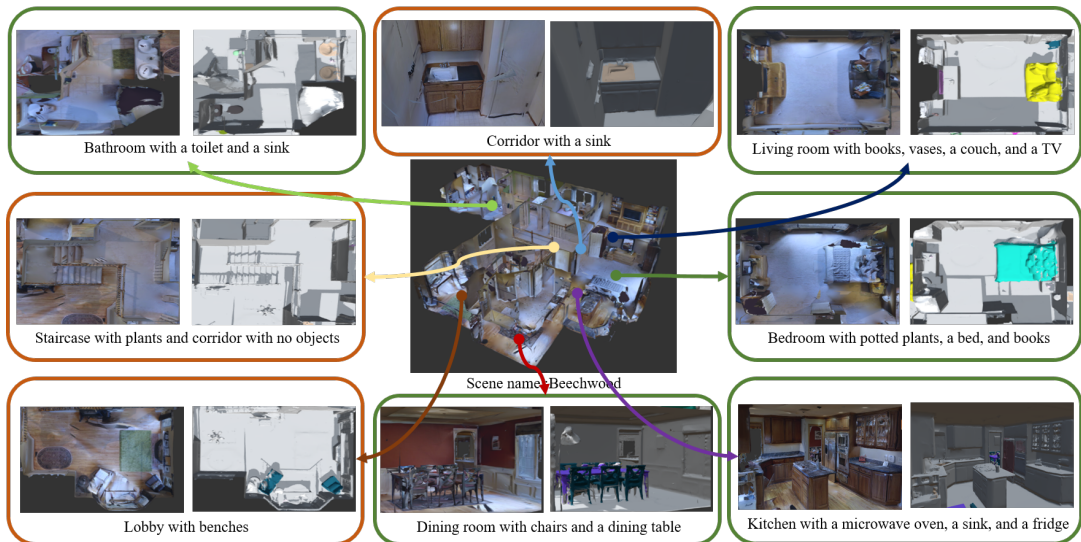


Fig. 4: A scene in the Stanford 3D Scene Graph dataset [5] where the point cloud representation, semantic mesh, and object information of various room segments are presented

is decided by the performance of the pose estimation and the mesh generation schemes which in our case have been thoroughly evaluated in [2] and [15], respectively. In the sequel, we focus on the semantic aspect of the 3DSGs and assess the performance of the proposed spatial perception approach.

B. Node description

The experiments shown in this section are mainly conducted with the Stanford 3D Scene Graph dataset “Klickitat” [5] corresponding to an expansive and complex indoor scenario of a three-floor residential building with 28 rooms and 112 objects. A 3DSG is available, whereas the raw data can be extracted using the iGibson environment [17] and used to supplement desired information to the 3DSG. The correctness, efficiency, and stability of the semantic search and the planning [9] are treated as evaluation criteria in these experiments.

Figure 5 and Figure 6 illustrate the results of semantic search in the case of different task queries when using 3DSG with and without detailed descriptions for object nodes of *Layer-2* and room nodes of *Layer-3*, respectively. The results demonstrate the enhanced semantic search efficiency when detailed node descriptions are included.

C. Room classification

This section presents the findings from the experiments with the room classification as a focus conducted using various LLMs and schemes developed along the investigation. For these experiments, we use the 35 scenarios of family apartment buildings in the Stanford 3D Scene Graph dataset [5] comprising 483 rooms and 2339 objects categorized in 35 types. The reason why we have turned to this dataset is twofold: first, it is a very large dataset encompassing representative and complex indoor household scenarios (cf. Figure 4 for an example); second, ground truth

Success

Fail

"floorB - kitchen - potted plant1": "This plant has long thorns."

"floorB - dining_room - potted plant2": "This plant has beautiful flowers."

"floorB - living_room2 - potted plant3": "This plant has dried up."

"floorB - living_room2 - potted plant4": "This is a green leaf plant."

- Find me a plant with thorns.

kitchen_B

Reasoning = The instruction is to find a plant with thorns. Memory shows that the kitchen, dining_room2, and living_room2 on floorB have been expanded. Among them, a potted plant with long thorns has been found in the kitchen on floorB. Therefore, the target object has been found, and the search is complete.
- Find me a plant that needs watering.

living_room2_B

Reasoning = The instruction is to find a plant that needs watering. Memory shows that the kitchen, dining_room2, and living_room2 on floorB have been expanded. Among these rooms, living_room2 has a plant that has dried up, indicating it needs watering. Therefore, the target plant has been found, and the search is finished.
- Find me a potted plant that is most likely a cactus.

kitchen_B

Reasoning = The instruction is to find a potted plant that is most likely a cactus. Memory shows that the kitchen, dining_room2, and living_room2 on floorB have been expanded. Among the potted plants found in these rooms, the one in the kitchen has node information indicating it has long thorns, which is a characteristic of a cactus. Therefore, I have found the target object and will set the mode to finish.

Fig. 5: Results of semantic search in the case of different task queries when using 3DSG with and without detailed object node descriptions, respectively

room labels are available in this dataset and can be taken as a reference for further evaluation. Hence, compared to the 3DSGs we have constructed in real-time in relatively limited scenarios, we believe using the dataset can better shed light on future development of room classification approaches based on LLMs.

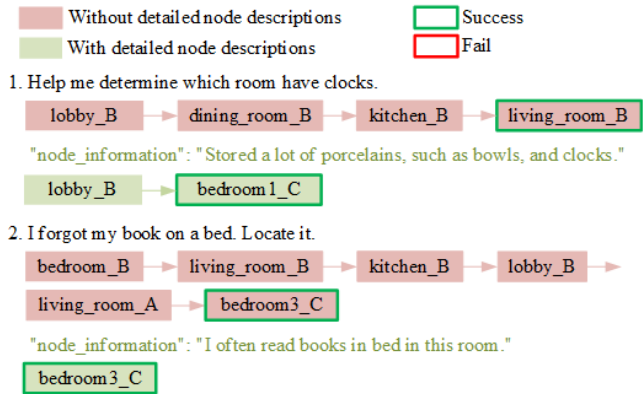


Fig. 6: Results of semantic search in the case of different task queries when using 3DSG with and without detailed room node descriptions, respectively

The initial approach involves querying the LLMs directly with information of the objects contained in the room node to identify the room category (cf. Figure 9(a) for an example). As presented in Table I, three distinct LLMs are tested: ERNIE-Speed-8K, KIMI-8K, and ERNIE-3.5-8K. The ERNIE-3.5-8K model, developed by Baidu Qianfan, demonstrates the highest accuracy, thus having been used for the subsequent analysis.

TABLE I: Accuracy of room classification when various LLMs and strategies are used

mode/method	accuracy	number of rooms annotated
ERNIE-Speed-8K	0.7060	483
KIMI-8K	0.7721	483
ERNIE-3.5-8K	0.8178	483
ERNIE-3.5-8K + polling	0.9527	358

In these initial experiments and analysis of these indoor household scenarios, we have checked the rooms for which the labels inferred by the LLM deviate from the ground truth given in the dataset [5], and we notice that not all segments of an indoor scenario can be well described with a single-word label, while some can be multi-functional. In addition, it is important to note that the rate of classification accuracy only measures the discrepancy between the estimated label and the ground truth label which technically cannot be regarded as absolutely right, for the label of a segment in an indoor scenario is not definite and can also be subjective. Therefore, our strategy is to not annotate all rooms with a single label, but to ensure that once a room label is given, it should be accurate. Multi-functional segments are captioned with a concise description. Typically, only room labels are provided for semantic search and task planning. If the room label field is empty, the node description is used instead.

Further investigation into the impact of object categories on room classification reveals significant disparities in accuracy across different object categories. As presented in Figure 7, rooms containing specific objects, such as “toilet”, show a perfect classification accuracy, implying that these

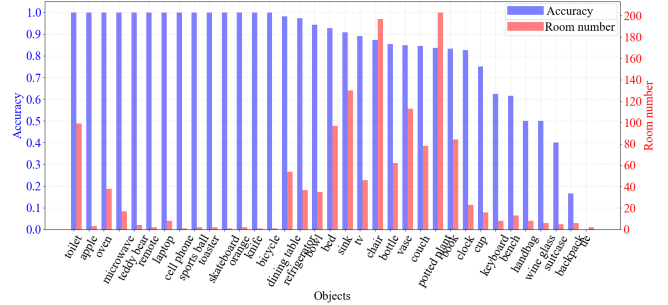


Fig. 7: Illustration of the impact of object categories on the accuracy of the room classification

objects can be treated as reliable indicators for room categorization.

The relationship between room categories and classification accuracy is also analyzed. Figure 8 shows that for certain room types, such as “dining room”, the classification accuracy is high. These rooms are then identified and used as the typical room labels in the polling approach introduced in Section II-B. An example is illustrated in Figure 9(b).

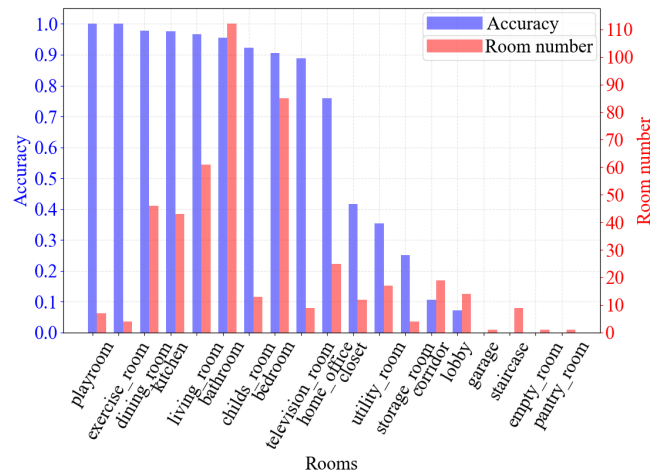
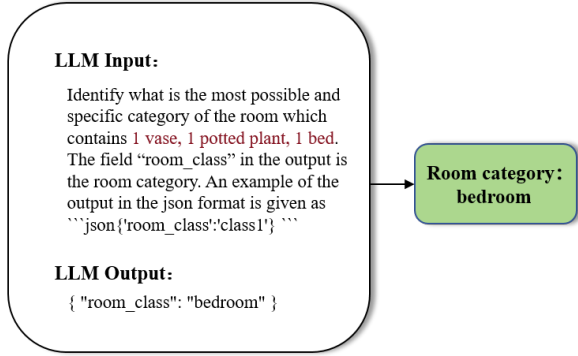
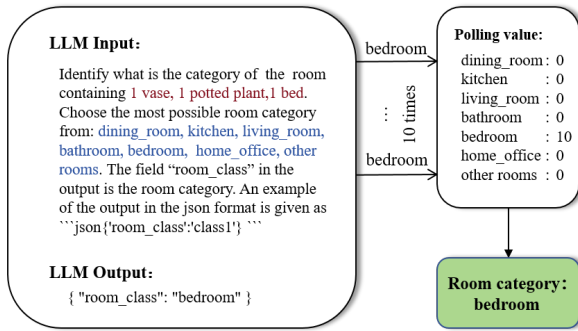


Fig. 8: Accuracy of the room classification with respect to room categories

The resulting enhanced accuracy of classification is presented in Table I. Only when the polling result is a “full-score” as illustrated in Figure 9(b), the room is captioned with the selected label. This strategy helps identify rooms with diverse object nodes and multiple functions for which a concise node description is more suitable and effective for subsequent robotic navigation tasks compared to a single room label. A few examples of such cases are shown in Table II. Therefore, the polling strategy proposed in this paper not only gives rise to an enhanced credibility of the resulting room label but also leads to an effective scheme of identifying and screening multi-functional segments of an indoor scenario. This intelligent “hybrid” room annotation method fully exploits the benefits of using LLMs and is tailored for complex indoor scenarios.



(a) Querying the LLMs directly with information of the objects contained in the room node



(b) With the polling strategy incorporated

Fig. 9: Illustration of two versions of the LLM-based room classification method and the prompts designed, with the node information that varies from node to node and the set of typical room labels that can be adjusted marked in a dark red and a light blue color, respectively

TABLE II: Examples of the polling results for multi-functional room segments

baseline	list of objects	polling results
home_office	1 bowl, 3 chairs, 3 potted plants, 1 laptop, 5 books, 1 clock, 3 vases	living_room: 5 bedroom: 5
bedroom	1 bench, 1 chair, 2 couches, 3 potted plants, 1 bed	living_room: 5 bedroom: 5
utility_room	1 backpack, 3 bottles, 2 cups, 1 chair, 4 potted plant, 1 sink	kitchen: 5 bathroom: 3 other room: 2
corridor	2 bowls, 1 vase	dining_room: 7 living_room: 2 kitchen: 1

IV. CONCLUSION

This research presents a significant advancement in the field of intelligent spatial perception for robotics by leveraging the power of LLMs to construct hierarchical 3DSGs. The proposed system has been validated through extensive experiments, demonstrating its effectiveness in generating accurate and comprehensive spatial representations for indoor environments. The innovative use of LLMs for node attribute generation and room classification has been shown

to enhance the semantic richness and scalability of 3DSGs, which are crucial for intelligent navigation and task planning. The polling mechanism introduced for room classification improves annotation accuracy and addresses the challenges of multi-functional room perception. The findings from this study lay a solid foundation for future research in 3DSG construction and the application of LLMs in robotics, paving the way for more sophisticated and context-aware intelligent agents.

REFERENCES

- [1] R. Mur-Artal and J. D. Tardós, “ORB-SLAM2: An open-source SLAM system for monocular, stereo, and RGB-D cameras,” *IEEE Transactions on Robotics*, vol. 33, no. 5, pp. 1255 – 1262, June 2017.
- [2] M. Labbe and F. Michaud, “RTAB-Map as an open-source lidar and visual simultaneous localization and mapping library for large-scale and long-term online operation,” *Journal of Field Robotics*, vol. 36, pp. 416 – 446, 2018.
- [3] F. Jiang, Y. Cheng, H. Wang, Z. Han, Y. Huang, F. Zhou, and J. Jiang, “An Engineering Solution for Multi-sensor Fusion SLAM in Indoor and Outdoor Scenes,” in the *43rd Chinese Control Conference (CCC 2024)*, Jul. 2024.
- [4] U.-H. Kim, J.-M. Park, T. jin Song, and J.-H. Kim, “3-D scene graph: A sparse and semantic representation of physical environments for intelligent agents,” *IEEE transactions on cybernetics*, vol. 50, no. 12, p. 4921–4933, 2019.
- [5] I. Armeni, Z.-Y. He, J. Gwak, A. Zamir, M. Fischer, J. Malik, and S. Savarese, “3D Scene Graph: A Structure for Unified Semantics, 3D Space, and Camera,” *2019 IEEE/CVF International Conference on Computer Vision (ICCV)*, pp. 5663–5672, 2019. [Online]. Available: <https://api.semanticscholar.org/CorpusID:203837042>
- [6] Q. Gu, A. Kuwajerwala, S. Morin, K. Jatavallabhula, B. Sen, A. Agarwal, C. Rivera, W. Paul, K. Ellis, R. Chellappa, C. Gan, C. de Melo, J. Tenenbaum, A. Torralba, F. Shkurti, and L. Paull, “ConceptGraphs: Open-Vocabulary 3D Scene Graphs for Perception and Planning,” *arXiv*, 2023.
- [7] N. Hughes, Y. Chang, S. Hu, R. Talak, R. Abdulhai, J. Strader, and L. Carlone, “Foundations of spatial perception for robotics: Hierarchical representations and real-time systems,” *The International Journal of Robotics Research*, 2024.
- [8] C. Agia, K. M. Jatavallabhula, M. N. M. Khodeir, O. Miksik, V. Vineet, M. Mukadam, L. Paull, and F. Shkurti, “TASKOGRAPHY:: Evaluating robot task planning over large 3D scene graphs,” in *Conference on Robot Learning*, 2022.
- [9] K. Rana, J. Haviland, S. Garg, J. Abou-Chakra, I. D. Reid, and N. Sünderhauf, “SayPlan: Grounding Large Language Models using 3D Scene Graphs for Scalable Task Planning,” in *Conference on Robot Learning*, 2023.
- [10] Z. Ravichandran, L. Peng, N. Hughes, J. D. Griffith, and L. Carlone, “Hierarchical representations and explicit memory: Learning effective navigation policies on 3D scene graphs using graph neural networks,” in *International Conference on Robotics and Automation (ICRA)*, 2022.
- [11] “GPT-4 Technical Report,” 2024.
- [12] H. Touvron, T. Lavril, G. Izacard, X. Martinet, M.-A. Lachaux, T. Lacroix, B. Rozière, N. Goyal, E. Hambro, F. Azhar, A. Rodriguez, A. Joulin, E. Grave, and G. Lample, “LLaMA: Open and Efficient Foundation Language Models,” *ArXiv*, 2023.
- [13] H. Liu, C. Li, Q. Wu, and Y. J. Lee, “Visual instruction tuning,” in *Advances in Neural Information Processing Systems*, A. Oh, T. Naumann, A. Globerson, K. Saenko, M. Hardt, and S. Levine, Eds., vol. 36. Curran Associates, Inc., 2023, pp. 34 892–34 916.
- [14] A. Radford, J. W. Kim, C. Hallacy, A. Ramesh, G. Goh, S. Agarwal, G. Sastry, A. Askell, P. Mishkin, and J. Clark, “Learning Transferable Visual Models From Natural Language Supervision,” in *International Conference on Machine Learning*, 2021.
- [15] A. Rosinol, M. Abate, Y. Chang, and L. Carlone, “Kimera: An Open-Source Library for Real-Time Metric-Semantic Localization and Mapping,” in *IEEE International Conference on Robotics and Automation (ICRA)*, Sept. 2020.
- [16] <https://github.com/ultralytics/ultralytics>.

- [17] B. Shen*, F. Xia*, C. Li*, R. Martin-Martin*, L. Fan, G. Wang, S. Buch, C. D'Arpino, S. Srivastava, L. P. Tchapmi, K. Vainio, L. Fei-Fei, and S. Savarese, "iGibson, a Simulation Environment for Interactive Tasks in Large Realistic Scenes," *arXiv preprint arXiv:2012.02924*, 2020.
- [18] A. A. Hagberg, D. A. Schult, and P. J. Swart, "Exploring Network Structure, Dynamics, and Function using NetworkX," in *7th Python in Science Conference*, 2008.
- [19] A. Rosinol, A. Violette, M. Abate, N. Hughes, Y. Chang, J. Shi, A. Gupta, and L. Carlone, "Kimera: From SLAM to spatial perception with 3D dynamic scene graphs," *The International Journal of Robotics Research*, vol. 40, pp. 1510 – 1546, 2021.